文章编号:1001-1595(2009)04-0311-08

Periodic Geocenter Motion Measured with SLR in 1993—2006

GUO Jinyun[1,2], CHANG Xiaotao[3], HAN Yanben[2], SUN Jialong[1]

1. College of Geodesy and Geomatics, Shandong University of Science and Technology, Qingdao 266510, China; 2. National Astronomical Observatories, Chinese Academy of Sciences, Beijing 100012, China; 3. Chinese Academy of Surveying and Mapping, Beijing 100039, China

由 SLR 观测的地心周期性运动(1993—2006 年)

郭金运[1,2], 常晓涛[3], 韩延本[2], 孙佳龙[1]

1. 山东科技大学 测绘学院, 山东 青岛 266510; 2. 中国科学院 国家天文台, 北京 100012; 3. 中国测绘科学研究院, 北京 100039

摘 要:地球质心(CM)是整个地球的质量中心,地心运动是由地球系统的质量重新分布激励的,特别是流体圈层。利用 SLR 对 LAGEOS 1/2 卫星的距离观测,解算 1993—2006 年期间的地心运动时间序列,然后分别利用小波变换和最小二乘法分析该序列,发现地心运动存在长期和周期性变化。地心的长期运动表明地壳形状在变化。季节性变化是地心运动的主项,主要是由地球流体圈层的质量分布造成的,如海洋、大气和陆地水等。地心运动还存在其他周期性和准周期性变化。地心运动存在 2～5 年的长周期变化。许多周期都存在渐变,这表明整个地球系统质量和环境存在不规则的变化。

关键词:卫星激光测距(SLR); 地心运动; 地球质量再分布; LAGEOS 1/2

Abstract: The center of mass of Earth (CM) is the center of total Earth's mass. The geocenter motion may be excited by the mass redistribution of Earth system, especially the fluid layer. A time series of geocenter motion measured with SLR on LAGEOS 1/2 is estimated and then analyzed with the wavelet transformation and the least squares method, respectively. The secular and periodic variations of geocenter motion are detected. The long-term movement indicates that the crustal figure is changing, the north hemisphere and 180-degree hemisphere are shrinking, and the south hemisphere and 0-degree hemisphere are swelling. The seasonal variations are the main components which may be caused from the mass distribution of Earth fluid layer, e. g. ocean, atmosphere and continental water. There are many other periodic or quasi-periodic variations. There are long periodic variations through 2 to 5 years. Many periods gradually change, which indicates that there exist nonregular fluxes for the environment and mass of the whole Earth system.

Key words: satellite laser ranging (SLR); geocenter motion; Earth mass redistribution; LAGEOS 1/2

中图分类号:P227　　**文献标识码**:A

基金项目:国际科技合作计划(2009DFB00130); 中国科学院对外合作重点项目; 国家高技术研究发展计划(2006AA12z303); 山东省泰山学者建设工程专项(TSXZ0502); 海岛(礁)测绘技术国家测绘局重点实验室基金(2009A02)

1 Introduction

The center of mass of Earth (CM) is the center of total Earth's mass, including the solid Earth and fluid layer, such as atmosphere, ocean and continental water. So CM is not identical to the center of mass of solid Earth (CE), and there exists a translation between them, which is called the geocenter motion (GCM)[1-2]. The origin of the terrestrial reference frame (TRF) is defined as CM at a special epoch. TRF can be realized and maintained with the space geodetic techniques[3]. CM is the physical center in the satellite dynamics. Therefore, GCM is not only one basic issue for the space geodesy and space science, but also is one important topic to built and maintain the international terrestrial reference frame (ITRF).

GCM may be mainly caused from the temporal variations of mass distribution for the fluid layer of Earth. So these geophysical variations can be observed and modeled to show GCM[4-5]. Based on the satellite dynamics, the coordinates of stations fixed on the crust can be solved from the satellite tracking observations to realize TRF. The origin of TRF, we all know, is CM at the observing epoch. So GCM relative to a reference position can be determined from the satellite tracking observations of these stations. Therefore the time series relative to a conventional origin measured with the space geodetic techniques such as the satellite laser ranging (SLR), the global positioning satellites (GPS), and the Doppler orbitography and radiopositioning integrated by satellites (DORIS), can also be used to determine GCM[6-7].

In the inertial space, CE can change its track when the mass of Earth redistributes. But the frame of CE cannot be directly observed. Otherwise the frame of CE is approximate to the frame of the center of Earth surface figure (CF). In the inertial space, CM is fixed relative to the satellite orbit in the dynamics. So the frame of CM is proper to SLR observations. Satellites rotation around CM can be observed from stations located on the crust. And the stations' coordinates are solved in ITRF, whose origin is the center in the geometric space, that is, CF. Because of the redistribution of Earth's mass, CM also differs from CF. The translation between them can be determined from the space geodetic observations to solve GCM[4-8]. Strictly speaking, GCM relative to CE is different from that relative to CF, but the difference is only about 2.1% [1].

There are two methods commonly used to explore GCM with the space geodetic technique[9]. One method is that degree one spherical harmonic expansion of the Earth gravity filed can be estimated at the observing epoch while fixing a TRF. Another method is that the time series of stations' coordinates is solved with the free-network method while fixing one Earth gravity field model. So a TRF series relative to a fixed TRF can be obtained.

A campaign of analysis on GCM was sponsored by the International Earth rotation and Reference system Service (IERS) in 1997—1998[10]. GCM in T_X, T_Y and T_Z directions detected by the space geodetic techniques is up to millimeter level. But the seasonal and secular variations of GCM explored from the space geodetic observations is submerged in errors after the diurnal and semi-diurnal tidal corrections are made with the tidal model, which indicates that GCM is small and the precisions for the space geodetic observations should be further improved. Meanwhile, GCM derived from the geophysical data is obviously dependent on the model, and not all frequencies appear in the geophysically-derived GCM series.

GCM has been ever studied using the space geodetic data and geophysical data, e.g. Dong, et al. with 1993—2002 GPS data[4-5], Chen, et al. with 1991—1997 SLR data[2], Bouillé, et al. and Crétaux, et al. with 1993—1998 DORIS data and SLR data[6,11], Wu, et al. with 1983—1994 SLR data[12]. These studies mostly intercompare the geophysically derived GCM prediction and use the geodetic data as the external evidence. The geodetic GCM is consistent to the geophysical GCM in the seasonal band. These studies show that the seasonal GCM may be owe to the mass redistribution of the fluid layer. SLR's GCM best matches the geophysical expectation in both amplitude and phase for the annual component, and DORIS's results are close to SLR's ones with exception of the amplitude in T_Y direction. The seasonal GCM derived from GPS is close to SLR's one in the equatorial plane exception for the amplitude and phase in T_Z direction.

The precision of SLR observation is up to millimeter level. GCM can be estimated with the satellite tracking data measured with SLR based on the dynamics[2]. To the global extent, SLR networks should be augmented. There is the space-time chaos to a certainty for the SLR under the effect of loading[13]. This paper aims to probe the capability of SLR to estimate GCM and study the secular and periodic variations of GCM, not how to solve GCM from SLR data.

2 Time series of GCM measured with SLR

LAGEOS, Laser Geodynamics Satellites, are a series of scientific research satellites designed to provide an orbiting laser ranging benchmark for geodynamical studies of the Earth. LAGEOS 1 was developed by NASA and was placed into a high inclination orbit to permit viewing by ground stations located around the world in May, 1976. LAGEOS 2 was a joint mission between NASA and the Italian Space Agency, and launched in Oct. 1992. The precision of SLR observations was only up to decimeter or centimeter level, and the distribution of SLR stations is asymmetrical around the world in 1980s. Since 1993, more SLR stations can meantime track LAGEOS 1/2 and the observing precision is up to 1 centimeter or millimeters[14-15].

Based on the satellite dynamics, a TRF series was estimated using the SLR tracking data on LAGEOS 1/2 in 1993—1996 from 86 stations around the world with the software of GINS/MATLO by Dr. Coulot D, et al. in Observatorie de la Côte d'Azur (OCA), France[14-16]. Coordinates of stations are firstly estimated with the free-network method to form a TRF series based on the satellite dynamics. Then the TRF series is transformed to ITRF 2000 with the 7-parameter model. Therefore a time series of TRF origins motion relative to ITRF 2000's origin is solved, which is a time series of GCM called OCA's GCM, seen in Fig. 1(a). There appear several spikes in T_X, T_Y and T_Z directions in Fig. 1(a), which shows that there are not only the secular and periodic components, but also some systematic and gross errors in OCA's GCM.

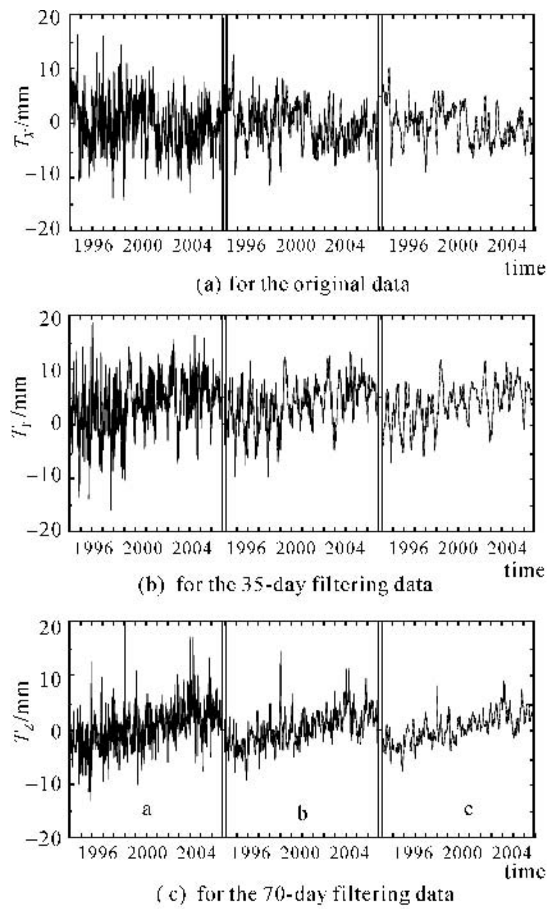

Fig. 1　GCM series measured with SLR

There are many errors in different bands for OCA's GCM under the effects of LAGEOS orbits, distribution of SLR stations, observing errors and solving strategy[15]. Feissel-Vernier, et al. ever analyzed the systemic errors for the SLR data[16]. Because more tidal effects are the high-frequency signals, the effects of diurnal and semi-diurnal tides are not considered for the SLR solution with 7-day arcs. The effects of satellite orbit on the station positions mainly have the periods of one cycle per revolution, right ascension, semi-annual and annual variations[17]. There are 17.5-day and 35-day systemic errors, and 14-day periodic error in T_Z for the LAGEOS orbits. Meantime, there is a 140-day bias in the SLR data. An interannual systemic error with 1 millimeter of amplitude for SLR data is made by the atmospheric loading[18]. A reference Earth gravity field model should be fixed to build a coordinate datum when the stations positions are solved. But the gravity model also includes errors in different bands which makes the solution to be of the annual error[19]. The error of coordinate transformation is also inducted when the TRF series are transformed to ITRF 2000 with 7-parameter model[20].

The seasonal variations are the main band in GCM by the analysis of space geodetic and geophysical data[5-6,10]. OCA's GCM is affected by not only the noise and high-frequency variations, but also the effects of periodic systematic and gross errors. In order to improve the signal-noise ratio of OCA's GCM, the series is filtered with the Gaussian filter to smooth the high-frequency components and detect the gross errors. The weighted function in the Gaussian filter is a normal-distributed function, which is

$$w(t,g)=\exp\left(-\frac{18r^2}{D^2}\right),\ r\leqslant\frac{1}{2}D \tag{1}$$

in which, D is a given searching window, and r is a distance to the centre point.

The window D directly affects the Gaussian filtering results. If the window is much large, the series may be excessively smoothed and take distortions. Otherwise, the origin series cannot be filtered and detected to find the gross errors. So it is very important to select an appropriate window. Considering the effect of LAGEOS orbits, the Gaussian filters are made with the 35-day and 70-day windows, respectively. Fig. 1(b) and 1(c) show the filtered OCA's GCM. Comparing the origin data and the filtered series, the filter can efficiently restrain the effect of noises and gross errors, and improve the signal-noise ratio. There appear large fluctuations for OCA's GCM in 1998, which may be disturbed by the El Niño that was strongest in the 20th century. Because we mainly pay attention to the seasonal and interannual variations of GCM, the time series of GCM after 70-day Gaussian filtering is used to study the periodic change of GCM. To evaluate the GCM measured with SLR, we compare it with the geocenter series used in ITRF2005 which is also filtered with the Gaussian filter. The root mean squares errors in T_X, T_Y and T_Z directions are 2.3, 2.6 and 4.5 mm, respectively.

3　Analysis on GCM variations with wavelet transform

GCM series measured with SLR to LAGEOS 1/2 in 1993—2006 after 70-day Gaussian filtering is analyzed with the Wvelet Transform (WT). WT is a signal-analyzed method in time and frequency domains with the variable resolutions[21]. Because the Morlet wavelet is a combination of trigonometric and Gaussian functions, it is widely used in geophysical and geodetic data analysis. Signals can be separated from noises in a time series by a wavelet filtering in a time and frequency domains, which can efficiently wipe off the effect of noises. Then a clean signal can be reconstructed and an ideal function can be gotten[22]. The wavelet analysis of GCM series measured with SLR is shown in Fig. 2, Fig. 3 and Fig. 4. The periods detected by WT are listed in Tab. 1. Fig. 2 ~ Fig. 4 also shows that these periods are temporally changing.

Fig. 2 Wavelet analysis of T_X variations

Fig. 3 Wavelet analysis of T_Y variations

Fig. 4 Wavelet analysis of T_Z variations

Tab. 1 Periods of GCM by WT

T_X	T_Y	T_Z
2 202.8	**2 202.8**	**2 202.8**
926.7	1 101.6	926.7
389.4	389.4	389.4
194.7	137.7	194.7

4 GCM temporal variations solved with least squares method

Supposing there is a time series $(t_i, g_i)(i=1,2,\cdots,n)$ of GCM which has the secular and periodic fluctuations. The long-term variation can be fitted with a polynomial, and the periodic term can also be fitted with a trigonometric function. Suppose there are m periodic terms, then

$$g_i = a + bt_i + \sum_{j=1}^{m}[c_j\cos(2\pi f_j t_i) + s_j\sin(2\pi f_j t_i)], i = 1,2,\cdots,n \tag{2}$$

where, a is a constant, b is the secular rate, and f_j is the frequency for the j-periodic term. The amplitude and phase of the j-periodic term are, respectively,

$$A_j = (c_j^2 + s_j^2)^{\frac{1}{2}},\ \varphi_j = \arctan\frac{c_j}{s_j} \tag{3}$$

There are $2+3m$ unknown parameters in equation (2). If only the sampling number satisfies $n \geqslant 2+3m$, the unknown parameters can be estimated with the least squares method. Equation (2) can be linearized with the Taylor series expansion, and expressed in matrix as

$$V = AX - W \tag{4}$$

where, $V = [v_1, v_2, \cdots, v_n]^T$ is the sampling correction vector, $X = [da, db, dc_1, ds_1, df_1, \cdots, dc_m, ds_m, df_m]^T$ is the unknown parameter vector, $W = [w_1, w_2, \cdots, w_n]^T$ in which $w_i = g_i - \left\{a + bt_i + \sum_{j=1}^{m} [c_j \cos(2\pi f_j t_i) + s_j \sin(2\pi f_j t_i)]\right\}$, and

$$A = \begin{bmatrix} 1 & t_1 & \overbrace{\cos(2\pi f_1 t_1) \quad \sin(2\pi f_1 t_1) \quad 2\pi t_1[s_1 \sin(2\pi f_1 t_1) - c_1 \cos(2\pi f_1 t_1)] \quad \cdots}^{3m} \\ \vdots & \ddots & \vdots \\ 1 & t_n & \cos(2\pi f_1 t_n) \quad \sin(2\pi f_1 t_n) \quad 2\pi t_1[s_1 \sin(2\pi f_1 t_n) - c_1 \cos(2\pi f_1 t_n)] \quad \cdots \end{bmatrix}_{n \times (2+3m)}$$

is the designed matrix. According to the least squares principle, the unknown parameter vector is estimated as

$$X = (A^T A)^{-1} A^T W \tag{5}$$

The estimated variance-covariance matrix for unknown parameters is

$$D_X = (A^T A)^{-1} \frac{V^T V}{n - 2 - 3m} \tag{6}$$

Equation (5) should be iteratively solved because there are errors for the given initial values and observations. There are the secular variation of GCM in T_X, T_Y and T_Z directions by the least square analysis, seen in Tab. 2. The periodic solutions are listed in Tab. 3. Not only a mean period within a time interval can be solved, but also its precision can be given with the least square analysis. The fluctuated range of the period can be further determined with the 3-sigma criterion, which indicates that the period may change. The period should be better called quasi-period under the excitations of many physical conditions. So the period and its changing interval can be solved from the sampling data in the least squares sense.

Tab. 2 Long-term change of GCM in the least squares sense

	T_X	T_Y	T_Z
constant/mm	1.48±0.17	0.64±0.14	−3.09±0.12
Rate/(mm/a)	−0.26±0.02	0.43±0.02	+0.50±0.02

Tab. 3 Periodic variations of GCM estimated with least squares method

T_X	period/d	882.9±9.0	372.1±0.8	301.3±2.5	243.2±1.2	182.3±0.5	123.9±0.2		
	amplitude/mm	1.2±0.2	2.3±0.2	0.5±0.2	0.6±0.2	0.8±0.2	0.9±0.1		
	phase/(°)	40.6±9.5	290.7±5.7	224.8±22.4	61.8±18.2	317.4±13.0	7.8±14.2		
T_Y	period/d	1 884.0±80.0	1 127.5±30.5	368.3±0.5	297.8±1.2	203.1±0.8	157.7±1.0	136.1±0.3	447.8±2.7
	amplitude/mm	0.5±0.1	1.0±0.3	3.5±0.2	0.8±0.1	0.6±0.1	0.6±0.3	0.7±0.1	0.9±0.1
	phase/(°)	359.3±23.6	135.3±19.3	312.6±2.8	190.1±13.6	170.9±19.2	214.2±33.4	164.5±16.1	205.5±12.0
T_Z	period/d	1 012.1±12.0	549.5±3.8	407.8±2.7	203.4±0.7	180.3±0.5	100.2±0.2		
	amplitude/mm	0.8±0.1	0.8±0.2	1.0±0.1	0.6±0.1	0.6±0.2	0.5±0.1		
	phase/(°)	99.2±12.0	235.0±10.6	291.5±16.4	67.7±16.7	28.9±13.8	262.5±19.5		

5 Discussions

5.1 Long-term change

GCM measured with SLR in 1993—2006 shows the visible secular variation, which is never covered before. The least square analysis gives the constants and rates of long-term variation in T_X, T_Y and T_Z directions, which obviously departs away zero. The rate in T_X direction is −0.26 mm/a that is different from ones in T_Y and T_Z directions, which are +0.43 mm/a and +0.50 mm/a, respectively.

The secular change rate in T_Z direction is largest and positive, which may be the response of the condensation of north hemisphere and the dilation of south hemisphere. This can make CF to move south relative to CM in the inertial space.

We all know that the 0-degree meridian hemisphere centered in the Atlantic called 0-degree hemisphere is of dissymmetry with the 180-degree meridian hemisphere centered in the Pacific called 180-degree hemisphere. There are regional dilatations in 0-degree hemisphere, and marginal shrinkages in 180-degree hemisphere by contraries. So these can make the secular rate in T_X direction to be negative. The T_X rate is negative, which indicates that CM moves to 180-degree hemisphere in the frame of CF.

The secular rate in T_Y direction is positive, which indicates that CM moves in the T_Y direction in the frame of CF. This may partially be excited by the condensation of 0-degree hemisphere and the dilation of 180-degree hemisphere. Otherwise, the largest change of atmospheric pressure appears in the middle Asia. The atmospheric variation in the middle Asia has a different phase with that in the Pacific and Atlantic. The solid Earth is a viscous elastomer. So the largest fluctuation of atmospheric pressure in the middle Asia can in part make the long-term rate in T_Y direction to be positive.

5.2 Seasonal variations

The seasonal variations that include the biannual and annual fluctuations are the main parts in GCM, which may be principally derived from the mass redistribution of atmosphere, ocean and continental water[2, 4, 9-10, 16, 23-24]. Seasonal variations are obviously all shown in the wavelet and least square analysis in this paper.

The WT analysis shows that there are the annual variation and semi-annual change in all three directions. The T_X, T_Y and T_Z annual period is 389 d. The T_X and T_Z semi-annual period is 195 d different from that in T_Y direction. A number of encouraging studies only showed that there are seasonal variations of GCM, but the idiographic periods are not given, e. g. [2, 4, 6, 11, 12, 16].

The least square analysis of GCM on the whole inosculates with the WT analysis. There are the annual variation in T_X and T_Y directions, whose periods are 372.1 d and 368.3 d, respectively, and phase difference is only 11.9°. These indicate that the annual fluctuation may have the same phase and be excited by the same physical phenomenon with the 3-sigma criterion. There is a quasi-annual change in T_Z direction, whose period is 407.8 d, which shows that the exciting physical mechanisms are different in the equinoctial and axis-rotating directions. But the T_Z phase is very close to the T_X phase, whose difference is only 0.8°. The annual variation in T_Z direction may be coupled with other periodic change of small amplitude. There are biannual variations in T_X and T_Z directions, whose periods are 182.3 d and 180.3 d, respectively. The semi-annual phase in T_X direction advances that in T_Z direction by 288.5°. But there is the quasi-semi-annual fluctuation in T_Y direction whose period is 203.1 d. The semi-annual phase in T_X advances that in T_Y by 146.5°.

There are obviously seasonal variations in T_X, T_Y and T_Z directions shown by the wavelet analysis. But the biannual and annual periods have a small fluctuation with 1 to 2 months. Speaking in this way, seasonal variations in T_X, T_Y and T_Z directions are all shown in the wavelet and least square analysis.

The least square analysis shows that the annual amplitude is larger than the biannual amplitude, e. g. 2.3 mm. vs. 0.8 mm in T_X, 3.5 mm. vs. 0.6 mm in T_Y and 1.0 mm. vs. 0.6 mm in T_Z, which is basically same as Lambeck's results about the effect of fluid layer on the Earth rotation[24]. The results are of little differences with the previous studies, e. g. [2, 5, 16]. They thought that the seasonal amplitude in T_Z direction is much lager than that in the equatorial plane. The difference is made by the solution and analysis method.

The seasonal GCM may be mainly caused from the mass redistribution of Earth surface fluid layer. The variation in the equatorial plane may be excited by the ocean, atmosphere, and in part continental water. The atmosphere acts on the ocean with the inverse-barometer effect so that it is difficult to partition the effect of atmosphere or ocean. The largest variation of atmospheric pressure appears in the middle Asia, which is a seasonal change[24]. This can make CM to vibrate in T_Y direction. There are another two largest variations of atmospheric pressure that take place in the north Pacific and the north Atlantic, respectively, which can make CM to vibrate in T_X direction. The seasonal motion in T_Z direction may be derived from the continental water exception for in part the atmosphere and ocean. Feissel-Vernier, et al. ever analyzed the spectral signal of Earth surface fluid with the Allen's variance method[16]. There are obvious annual fluctuations for the continental water in T_X, T_Y and T_Z directions, and there are seasonal and non-seasonal variations in the oceanic and atmospheric spectrums. The excitation of atmosphere and ocean is of white noise in the equatorial plane, and that in T_Z direction is of flicker noise.

5.3 Other periodic variations

A period of 407.8 d in T_Z is estimated in the least square analysis. This is a quasi-annual variation. Considering the effect of solid inner core, fluid outer core, elastic mantle, self-gravitation, and radial variation of density and rigidity in the core, Smith ever gave the contribution of core and mantle to the Earth wobble, whose period is 405.2 d [25]. This period inosculates with the period of 407.8 d in T_Z by the least square analysis.

A period of 549.5 d in T_Z is shown in the least square analysis. Lambeck ever showed that there is a period of 545 d for the polar tide of atmosphere[24], which is very close to 549.5 d given in the paper.

By the least square analysis, periods of 882.9 d in T_X, of 1 127.5 d and 1 884.0 d in T_Y, of 1 012.1 d in T_Z are shown. This indicates that there are long periodic variations in GCM.

The periodic variations with periods of 301.3 d and 297.8 d in T_X and T_Y, respectively, are found by the least square analysis, but their phases are not same with the difference 34.7°.

There are periodic fluctuations with period of 243.2 d in T_X, 203.1 d in T_Y and 203.4 d in T_Z in the least square analysis. The periods in T_Y and T_Z are very near, but their phases are clearly different. The phase of the period in T_X is very close to that in T_Z.

There are many other signals with different bands with exception of the above secular and periodic variations in the GCM series measured with SLR, which should be further lucubrated in the future.

6 Conclusions

The GCM time series is estimated from the SLR data to LAGEOS 1/2 in 1993—2006. The secular and periodic variations of GCM measured with SLR are detected with the wavelet transformation and the least square method, respectively. The long-term movement of GCM indicates that the crustal geometric figure is changing in the inertial space. This may be derived from the glacial rebound, sea level rising, global warming, human activities and so on.

The seasonal variations are the main component which may be caused from the mass distribution of Earth fluid layer. There are many other periodic or quasi-periodic variations. Of course, there are long periodic variations through 2 to 5 years. Many periods gradually change, which are called quasi periods. This indicates that there exist nonregular fluxes for the environment and mass of the whole Earth system.

The graduate change of period can be explored by the wavelet analysis. The least square analysis can show the varying range of period. Therefore, the two methods can be together used to efficiently analyze the secular and periodic variations of GCM. Meanwhile, the Gaussian filtering can improve the signal-noise rate of GCM series.

Acknowledgements: The authors thank Dr. Berio P. and Coulot D. in Observatorie de la Côte d'Azur, France, for their helpful proposals, and are grateful to the anonymous reviewers for their proposals. The authors thank the International Laser Ranging Service (ILRS) for releasing SLR data.

References:

[1] BLEWITT G. Self-consistency in Reference Frames, Geocenter Definition and Surface Loading of the Solid Earth [J]. J Geophys Res, 2003, 108(B2): 2103.

[2] CHEN J L, WILSON C R, EANES R J, et al. Geophysical Interpretation of Observed Geocentre Variations[J]. J Geophys Res, 1999, 104(B2): 2683-2690.

[3] ALTAMIMI Z, BOUCHER C, SILLARD P. ITRF2000: A New Release of the International Terrestrial Reference Frame of Earth Science Applications[J]. J Geophys Res, 2002, 107(B10): 2214-2232.

[4] DONG D N, DICKEY J O, CHAO Y, et al. Geocenter Variations Caused by Atmosphere, Ocean and Surface Ground Water[J]. Geophys Res Lett, 1997, 24(15): 1867-1870.

[5] DONG D N, YUNCK T, HEFLIN M. Origin of the International Terrestrial Reference Frame[J]. J Geophys Res, 2003, 108(B4): 2200-2209.

[6] BOUILLE F, CAZENAVE A, LEMOINE J M, et al. Geocenter Motion from the DORIS Space System and Laser Data to the Lageos Satellites: Comparison with Surface Loading Data[J]. Geophys J Int, 2000, 143(1):71-82.

[7] WU X, ARGUS D F, HEFLIN M B, et al. Large-scale Global Surface Mass Variations Inferred from GPS Measurements of Load-induced Deformation[J]. Geophys Res Lett, 2003, 30(14): 1742-1745.

[8] CHENG M, TAPLEY B D. Variations in the Earth's Oblateness during the Past 28 Years[J]. J Geophys Res, 2004, 109: B09402, doi:10.1029/2004JB003028.

[9] GUO J Y, HAN Y B, HWANG C W. Analysis on Motion of Earth's Center of Mass Observed with CHAMP Mission [J]. Science in China: G, 2008, 51(10): 1597-1606.

[10] RAY J. IERS Analysis Campaign to Investigate Motions of the Geocenter[C]//IERS Technical Note 25. Paris: Observatoire de Paris, 1999.

[11] CRÉAUX J F, SOUDARIN L, DAVIDSON F J M, et al. Seasonal and Interannual Geocenter Motion from SLR and DORIS Measurements: Comparison with Surface Loading Data[J]. J Geophys Res, 2002, 107(B12): 2374-2382.

[12] WU B, PENG B B, XU H Z. Determination of Geocenter Motion[J]. Chin Sci Bull, 1999, 44(16): 1517-1519.

[13] VAN DAM T M, WAHR J, MILLY P C D, et al. Crustal Displacements due to Continental Water Loading[J]. Geophys Res Lett, 2001, 28: 651-654.

[14] COULOT D. SLR and Combinations of Space-geodetic Solutions: Contribution to reference Systems[D]. Paris: Paris Observaotry, 2005.

[15] GUO J Y, HAN Y B. Seasonal and Inter-annual Variations of Length of Day and Polar Motion Observed by SLR in 1993—2006[J]. Chinese Science Bulletin, 2009, 54(1): 46-52.

[16] FEISSEL-VERNIER M, LE BAIL K, BERIO P, et al. Geocentre Motion Measured with DORIS and SLR, and Predicted by Geophysical Models[J]. J Geod, 2006, 80: 637-648.

(下转第 329 页)